Observation of H-Mode Confinement in the DIII-D Tokamak with Electron Cyclotron Heating

John Lohr, B. W. Stallard,[a] R. Prater, R. T. Snider, K. H. Burrell, R. J. Groebner, D. N. Hill,[a] Kyoko Matsuda, C. P. Moeller, T. W. Petrie, H. St. John, and T. S. Taylor

General Atomics, San Diego, California 92138

(Received 29 October 1987)

The first observation of H-mode confinement with electron cyclotron heating as the sole auxiliary heating method has been made in divertor discharges in the DIII-D tokamak. These discharges exhibit the usual characteristics of the H mode, including improved confinement of particles and energy, when electron cyclotron heating is added at a power level above 0.7 MW. The H-mode transition is accompanied by the development of an electron temperature pedestal of 0.25 keV and a dramatic steepening of the density gradient near the separatrix.

PACS numbers: 52.55.Fa, 52.50.Gj

The plasma energy-confinement time in tokamaks has generally been found to decrease when auxiliary power is added to the Ohmic heating. This phenomenon, L-mode scaling,[1] makes it difficult to heat a tokamak plasma to reactor temperatures. However, a regime of improved confinement, H-mode scaling, has been observed in several tokamaks with neutral-beam injection (NBI) heating.[2-7] In the H mode, the energy confinement time may remain at the Ohmic level without degradation when auxiliary power is added, or the confinement time may degrade with power but remain a factor of about 2 larger than the confinement time under the L-mode scaling, as in the JET tokamak.[7] Recently, the H mode has also been obtained with ion cyclotron heating,[8] and, in the JFT-2M tokamak, with ion cyclotron heating,[9] with a combination of NBI and electron cyclotron heating (ECH),[10] and with NBI in limiter discharges.[11] The present work reports the first observation of the H mode with electron cyclotron heating as the sole source of auxiliary heating.

These experiments have been carried out in the DIII-D tokamak operated in the expanded boundary divertor configuration under conditions which have facilitated the H-mode transition in discharges heated by NBI.[5,12] Typical plasmas had $R_0 = 1.68$ m, $a = 0.62$ m, elongation $= 1.8$, with a single null divertor located in the direction of the ion ∇B drift, as preferred for the H mode.[13] The gap between the separatrix flux surface and the nearest material wall was typically 3.5 cm. The plasma was developed from deuterium gas, and the plasma current was 0.48 MA.

The ECH power was applied at a frequency of 60 GHz, for which the second-harmonic resonance occurs at a local magnetic field of 1.07 T. The antennas were located near the outside midplane of the plasma, and launched 85% of the incident power in the extraordinary mode and 15% in the ordinary mode. The total incident power, after allowance for waveguide losses, was up to 0.9 MW. The antennas launch power in the HE_{11} mode at an angle $\pm 17°$ to the radial with a Gaussian dispersion 11° in half width. When the resonance is at the plasma center, for the 17° launch angle, the local cutoff density for the extraordinary mode is 1.86×10^{19} m^{-3}, and for densities well below cutoff, the power is deposited in a volume with approximate minor radius of 20 cm in the midplane. The ECH power was typically a factor of 8 larger than the Ohmic power during the heating, and so the plasma power balance was dominated by the auxiliary heating.

The signatures of the H-mode transition are an increase in the plasma energy, signifying an improvement in the global energy-confinement time τ_E; an increase in the plasma density and a decrease in the D_α emission, indicating an improvement in particle-confinement time τ_p; and a broadening of the pressure profile. All of these characteristics were observed in the ECH H-mode discharges, of which the data in Fig. 1 are typical. The L-mode phase of this discharge lasted for 70 ms after ECH initiation. Then the discharge entered the H-mode phase.

At the H-mode transition, the density began to increase. At the same time, the D_α light emission from the plasma midplane decreased [Fig. 1(e)]. (D_α emission also dropped in the divertor region.) This behavior indicates a sudden increase in particle-confinement time of the plasma within the separatrix. Just after the transition, the line-averaged density rose at the rate of 4.4×10^{19} m^{-3} s^{-1}, which is the same rate found after the transition when the power source is NBI at the 1.8-MW power level. Unlike NBI, ECH injects no particles; therefore the density rise does not require particles from the heating source.

The discharge of Fig. 1 went through two complete H-mode cycles. In the first, it remained in the H mode for about 150 ms and then reverted to L mode. Ray-tracing calculations show that the reverse transition from H to L mode occurred when the density had risen to levels for which the absorption of the ECH power in a single pass had dropped to < 0.5 MW because of refraction, and the plasma center was cut off for most rays. In

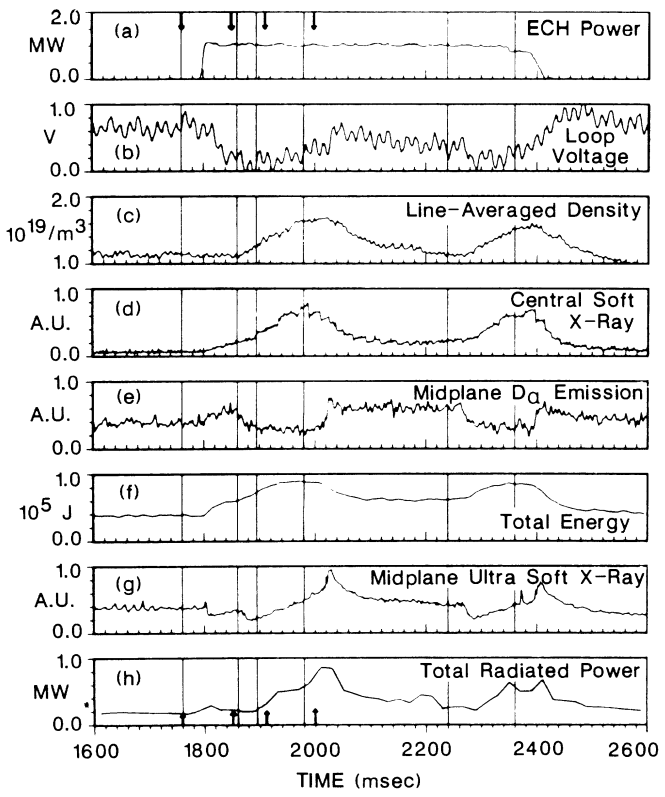

FIG. 1. Data from discharge number 56360 with 0.48-MA plasma current, and toroidal field of 1.07 T. Traces labeled A.U. are in arbitrary units. The vertical lines are the times of energy analysis of Table I; arrows indicate the times corresponding to the profiles of Fig. 2.

addition, the power radiated from within the separatrix [Fig. 1(h)] had increased to 0.8 MW, 90% of the incident ECH power. During the L mode, which started near 2020 ms, the particle confinement was poorer than in H mode, and the density decayed to well below the cutoff value. The time of the second H-mode transition appears to have been determined by the power balance. Although the density was below cutoff, the second transition to the H mode was prevented until the radiated power dropped to near its L-mode level of 0.3 MW. Measurements of the total radiated power and of power flux to the divertor show that despite less than 50% calculated first-pass absorption during the H mode, most of the ECH power is absorbed somewhere in the plasma, probably near the edge following multiple reflections from the wall.

The plasma energy, W, calculated from a full MHD equilibrium analysis [Fig. 1(f)] showed an improvement in global τ_E when the H-mode phase was entered. The increase in energy due to the addition of the ECH power had saturated in the L-mode phase by 1860 ms. At the transition, the time derivative of the energy abruptly increased, with dW/dt equal to about 0.35 MW. The energy rose to a peak value of 89 kJ from 60 kJ in the L-mode phase and 39 kJ in the Ohmic phase. Stored energy values determined from measurements of the plasma diamagnetism agree with the MHD analysis values within the uncertainty of ± 0.05 in β_p.

Determination of τ_E for these phases is complicated by the absence of a steady state in the H mode. Although $dW/dt=0$ several times during the evolution, other signals—for example, the radiated power—were not constant. In this paper, only the gross energy-confinement time $\tau_E = W/(P_\Omega + P_{\rm ECH} - dW/dt)$ is presented, where P_Ω is the Ohmic power and $P_{\rm ECH}$ includes all the microwave power incident on the plasma. In Table I, τ_E values are presented. When the dW/dt correction is included, nearly the full Ohmic τ_E is recovered early in the H mode when the ECH power is expected to have strong single-pass damping. At 1980 ms, when $dW/dt=0$, despite the impaired damping at higher density, τ_E was still 70% of the Ohmic value. These values were obtained again during the second H-mode cycle.

The effects of the H-mode transition on plasma density and temperature can be seen in Fig. 2. The ECH resulted in increased electron temperature during the L mode, with little change in the density. Following the H-mode transition, a further increase in T_e including a 250-eV edge pedestal occurred before the density had risen to levels for which deposition of the power near the plasma center was decreased [Fig. 2(c)]. Later in the H mode, the central electron temperature dropped [Fig. 2(d)] presumably because of reduced power to the plas-

TABLE I. Gross energy-confinement time τ_E, plasma energy W, rate of increase of energy $\dot{W}$, and line-averaged density in units of 10^{19} m^{-3}, at different times of discharge 56360 of Fig. 1. The ECH power launched was 0.9 MW. For the 2360-ms entry, although one gyrotron had tripped off, the full power was used in the τ_E calculation.

	t (ms)	Phase	$\bar{n}_e$	W (kJ)	$\dot{W}$ (MW)	τ_E (ms)
1	1760	Ohmic	1.1	39 ± 7	0	133 ± 24
2	1860	L mode	1.1	60 ± 7	0	55 ± 6
3	1895	H mode	1.3	70 ± 7	0.35 ± 0.1	120 ± 24
4	1980	H mode	1.6	88 ± 7	0	92 ± 7
5	2240	L mode	1.1	61 ± 7	0	57 ± 7
6	2360	H mode	1.5	87 ± 7	0	87 ± 8

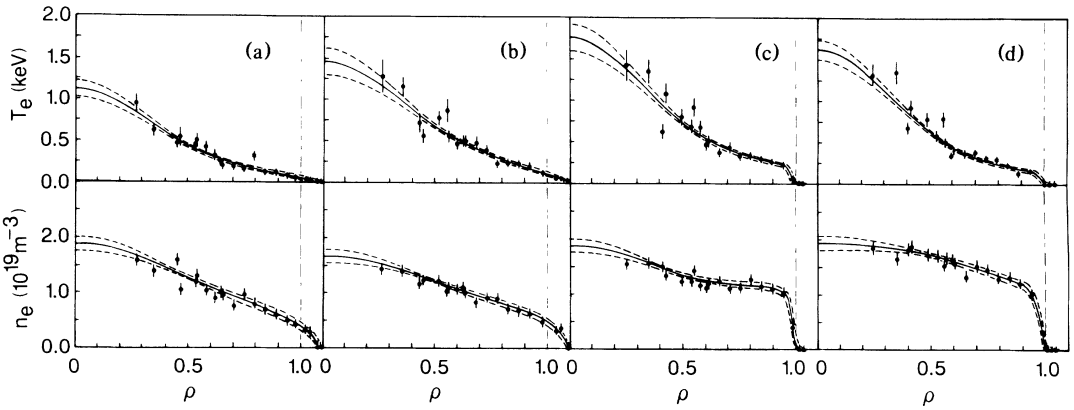

FIG. 2. Electron temperature and density profiles from Thomson scattering taken at different times in the evolution of reproducible discharges under conditions identical to those of Fig. 1. The profiles are taken at the times indicated by arrows in Fig. 1: (a) in the Ohmic phase; (b) near the end of the L-mode phase; (c) after the H-mode transition; and (d) near the end of the H-mode phase. The abscissa, ρ, is the normalized flux coordinate, with the separatrix flux surface ($\rho=1$) identified by the vertical dashed lines. The other dashed lines represent the propagated uncertainties in the fitting procedure.

ma center caused by increased density. The density profile became extremely flat in the H mode with a very large density gradient at the edge of the profile. These electron profile effects are also characteristic of NBI H modes in DIII-D and suggest that a steep edge pressure gradient rather than an edge electron temperature pedestal as previously reported[14] may be a key characteristic of the H mode.

ECH appears to be more effective in the attainment of the H mode than NBI heating at the same power level. In order to compare ECH and NBI most directly, heating experiments were performed with neutral injection at powers comparable to the ECH power, into reproducible discharges similar to that of Fig. 1. With 1.8 MW of 70-kV deuterium neutrals, an H-mode transition very similar to that of Fig. 1 was observed. When the absorbed NBI power was reduced to 1 MW by our decreasing the accelerating voltage to 60 kV, the H-mode transition required 300 ms of NBI pulse before it occurred. Power-deposition calculations verified that the heating profile was only slightly affected by the change in beam energy.

The data in Fig. 3 summarize the results of scanning of the ECH resonance in major radius. Figure 3(a) shows that when the resonance was located outside $r/a \cong 0.4$, the H mode was not attainable at the 0.9-MW power level, although the transition was highly reliable at that power level when the resonance was more central. In Fig. 3(b) the delay Δt_H between the start of the heating and the H-mode transition is plotted as a function of the resonance radius. The quantity Δt_H has been found in NBI discharges to be a decreasing function of injected power, and may be regarded as a measure of the strength of the transition in ECH experiments at constant power. Figure 3(b) shows that the transition delay becomes longer (i.e., the transition becomes weaker) as the reso-

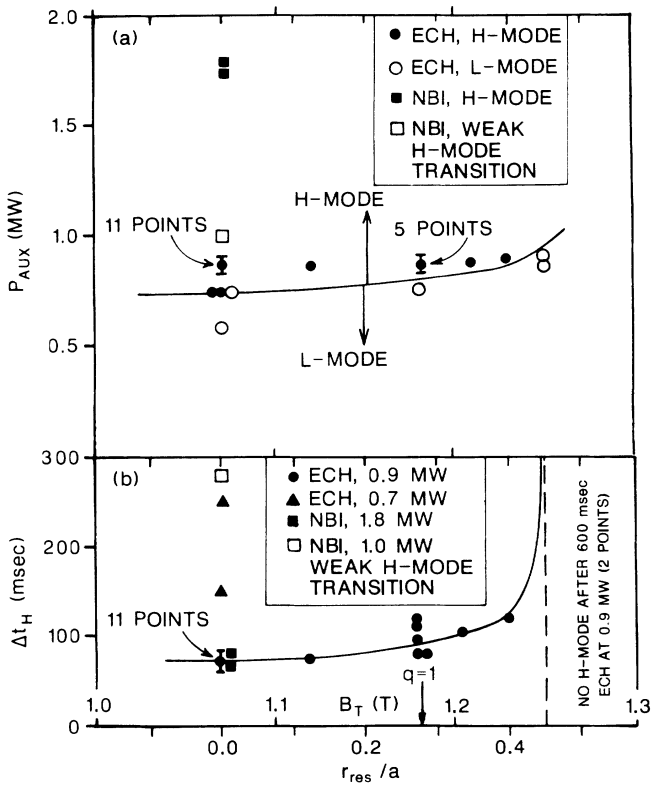

FIG. 3. (a) The region of parameter space where the H mode is found. The horizontal axis is the toroidal magnetic field, which determines the minor radius of the ECH resonance, r_{res}/a. The vertical axis is the auxiliary power. Open circles are L mode and the filled circles are H mode. The open square is for 1-MW NBI, for which the transition was weak, and the filled squares are for H-mode discharges with 1.8 MW of NBI. (b) Delay time Δt_H between the start of the heating and the transition to H mode, as a function of toroidal field. Filled symbols indicate H-mode discharges.

nance is moved outward or the power is reduced.

Power deposition profiles with neutral injection are inherently broader than with ECH. The more central localization possible with ECH may be the reason for its higher efficiency in obtaining the transition. However, because the radial scan of the ECH resonance was accomplished by variation of the toroidal magnetic field, it is impossible to be certain that an increase in the power threshold with field was not responsible for the trends illustrated in Fig. 3. On DIII-D, NBI data suggest that the H-mode threshold increases at most linearly with toroidal field. Observations on JET[15] also indicate that the threshold power increases with field. In the present work the field was varied by 20% and the power threshold increased by 20% as the resonance was scanned, consistent with the NBI results. Future work will address this question.

In summary, we have observed the improved confinement properties of the H mode in divertor discharges in which electron heating by ECH is the sole auxiliary heating. These discharges exhibit the characteristics of the H mode found with neutral injection or ion cyclotron heating, including improved particle and energy confinement. The physics of the H mode and, in particular, the gross behavior of the density are not strongly dependent on the heating method. These results support the application of ECH to plasma heating in the next generation of tokamaks.

The authors are grateful for discussions with M. Ali Mahdavi, T. C. Simonen, and R. D. Stambaugh, to J. C. DeBoo, P. Gohil, C. L. Hsieh, and R. E. Stockdale for the Thomson scattering data, and for excellent work by W. P. Cary and J. F. Tooker operating and maintaining the gyrotrons.

This work was supported by the U.S. Department of Energy under Contract No. DE-AC03-84-ER51044.

---

[a]Permanent address: Lawrence Livermore National Laboratory, Livermore, CA 94550.

[1]S. M. Kaye and R. J. Goldston, Nucl. Fusion **25**, 65 (1985).

[2]F. Wagner *et al.*, Phys. Rev. Lett. **49**, 1408 (1982).

[3]S. M. Kaye *et al.*, J. Nucl. Mater. **121**, 115 (1984).

[4]J. C. DeBoo *et al.*, Nucl. Fusion **26**, 211 (1986).

[5]J. Luxon *et al.*, in *Proceedings of the Eleventh International Conference on Plasma Physics and Controlled Nuclear Fusion Research, Kyoto, Japan, July 1986* (Vienna, 1987), p. 159.

[6]K. Odajima *et al.*, in Ref. 5, p. 151.

[7]A. Tanga *et al.*, in Ref. 5, p. 65.

[8]K. Steinmetz *et al.*, Phys. Rev. Lett. **59**, 124 (1987).

[9]H. Matsumoto *et al.*, Nucl. Fusion **27**, 1181 (1987).

[10]K. Hoshino *et al.*, Japanese Atomic Energy Research Institute Report No. JAERI-M-87-096, 1987 (unpublished).

[11]S. Sengoku *et al.*, Phys. Rev. Lett. **59**, 450 (1987).

[12]K. H. Burrell *et al.*, Phys. Rev. Lett. **59**, 1432 (1987).

[13]F. Wagner *et al.*, Nucl Fusion **25**, 1490 (1985).

[14]M. Keilhacker *et al.*, Plasma Phys. Controlled Fusion **28**, 29 (1986); K. Hoshino *et al.*, J. Phys. Soc. Jpn. **56**, 1750 (1987).

[15]A. Tanga *et al.*, Nucl. Fusion **27**, 1877 (1987).